USE OF THE METHOD OF PHOTOCHROMIC VISUALIZATION TO STUDY THE CONSTRAINED FLOW OF A VISCOUS FLUID IN A PIPE

Yu. S. Rayzantsev and V. N. Yurechko

UDC 532.574.8

This article reports results of a study of the structure of a steady flow of fluid in a circular pipe of constant cross section in the presence of an obstacle of complex form. The results were obtained by the method of photochromic visualization (PCV) [1-3]. In this method, information on the motion of the fluid is based on observations of displacements of colored markings induced by ultraviolet radiation in an initially colorless liquid serving as the solvent for a photochromic substance [2]. A description is given below of the unit and the method used to record the motion of the photochromic markers in the fluid with an improved RFK-5 pull-down type motion-picture camera at a speed of up to 100 frames/sec. The modifications include a substantial reduction in the period of film acceleration and monitoring of the operating regime during the entire period of filming. The goal of this study was to prove that the PCV method can be used to analyze the structure of hydrodynamic flows in channels with a complex geometry (to determine the localizations of the eddy and stagnant zones, separation points, etc.). Thus, we placed an obstacle consisting of two half-disks in a cylindrical channel so that the upper half-disk was parallel to the pipe axis and the lower half-disk covered half the cross section of the pipe and formed a slit with the other half-disk. We studied the velocity field for a steady flow regime.

We used a test stand on which the steady-state velocity field was created on a horizontal section in front of the obstacle. Since the discharges at which flow in the pipe becomes unstable are determined by the characteristics of the stand (pipe length, roughness of the inside surface of the pipe, pump pulsations, etc.) and the velocity field in front of the obstacle has a significant effect on the structure of the flow behind the obstacle, along with recording the velocity field after the obstacle we arranged for visualization of the velocity profile of a flow in a circular pipe at different discharges.

Figure 1 shows a diagram of the hydrodynamic stand, where 1 is a collection tank; 2, 3, and 10 are outlet values; 4 is a damper, 5 and 9 are metal pipes; 6 and 8 are pressure sensors; 7 is the working section – a tube of organic glass; 11 is a flexible hose; 12 and 15 are control valves; 13 is a centrifugal pump; 14 is a rotameter; 16 is an oscillograph; and 17 is a mercury thermometer. The centrifugal pump moved the working photochromic solution through the system. The discharge of the solution was regulated by changing the voltage supplied to the electric motor and by the use of control valves. The solution discharge was kept constant to within ±2%. To alleviate optical distortions, the working section of the pipe was placed in a rectangular tray filled with distilled water.

To create the colored markings, we used the second-harmonic radiation from solid ruby lasers. The equipment used to create and record the colored markings in the working section of the stand is shown schematically in Fig. 2, where 1 and 2 are the solid-state lasers; 3 and 5 are quartz prisms; 4 is the cross section of the fluid channel; 6 is the film lamp; 7 is a heat filter; 8 is a matted diffuser screen; 9 is the recorder; 10 is a 15-27 pulse generator; 11 is an I1-8 time-shift source; 12 is the control panel of the unit; and 13 are cylindrical quartz lenses. The use of two lasers, located next to each other, made it possible to create colored markings in two cross sections. Here, the G5-27 pulse generator supplied the lasers with two synchronous or time-shifted trigger pulses. The second harmonic, with λ = 347 nm, was separated in KDP crystals [4]. Here, the solid-state lasers were operated in a regime characterized by regular pulsations of constant intensity in order to allow more efficient conversion to the second harmonic [4]. This operating regime made it possible to increase conversion efficiency by a factor of two or three compared to the scheme employed in [2]. In that study investigators used a master laser, with subsequent amplification and conversion to the second harmonic in KDP crystals.

Moscow. Translated from Zhurnal Prikladnoi Mekhaniki i Tekhnicheskoi Fiziki, No. 5, pp. 14-19, September-October, 1987. Original article submitted June 4, 1986.

 0021-8944/87/2805-0654$12.50

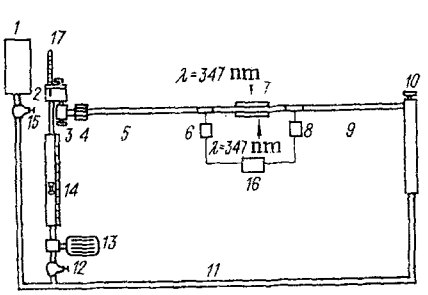

Fig. 1

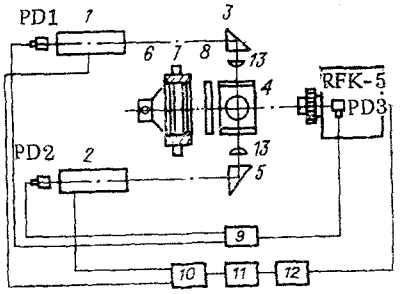

Fig. 2

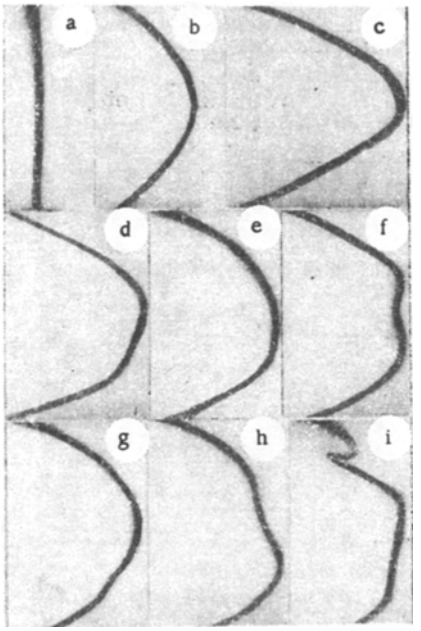

Fig. 3

The scheme proposed here for obtaining $\lambda = 347$ nm is simpler, although it was necessary to increase the length of the pulse to $\tau = 8 \cdot 10^{-4}$ sec, versus $\tau = 50 \cdot 10^{-9}$ sec in [2]. The movement of the colored markings was recorded with an RFK-5 camera operated in the frequency regime at a speed of 100 frames/sec. This speed was achieved by changing the gear ratio of the reduction gear which transmits rotation from the electric motor of the camera to the electromagnetic coupling which activates the film-winding mechanism. The trigger times of the single-pulse lasers were determined by signals from photodiodes installed on the resonators of the lasers. Another photodiode was installed in the camera to receive a light signal through the film from an external light source at the moment the film gate opens. The signals from the photodiodes went to the recorder, which then recorded the time between frames, the shutter speed, and the trigger times of the lasers. A synchronization system ensured that the lasers were triggered the moment the camera reached a constant speed. The time of camera acceleration was 0.03 sec.

To eliminate heating of the working part of the fluid channel, we added a heat filter to the bias lighting system. The filter contained a pumpable solution of copper sulfate. The walls of the filter were made of organic glass. The concentration of copper sulfate in distilled water was 0.3 moles/liter, while the optimum pumping rate was 0.2 liters/min. The dependence of the optical density of a heat filter with a 10-mm-thick layer of solution on the wavelength was obtained on an SF-26 spectrophotometer in [5]. The use of a heat filter made it possible to eliminate heating of the working medium by the lamp and to increase the contrast of the colored marking and the lifetime of the photo-induced colored markings, which decreases with an increase in temperature.

Focusing of the laser radiation with cylindrical quartz lenses in the working section created wedge-shaped colored markings. The dimensions of these markings in the plane of

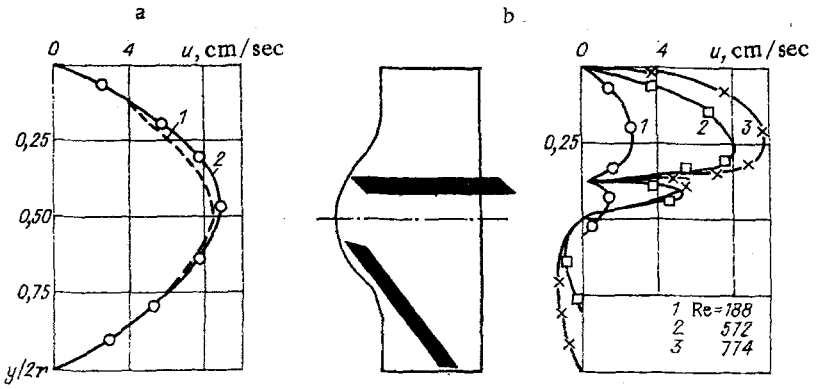

Fig. 4

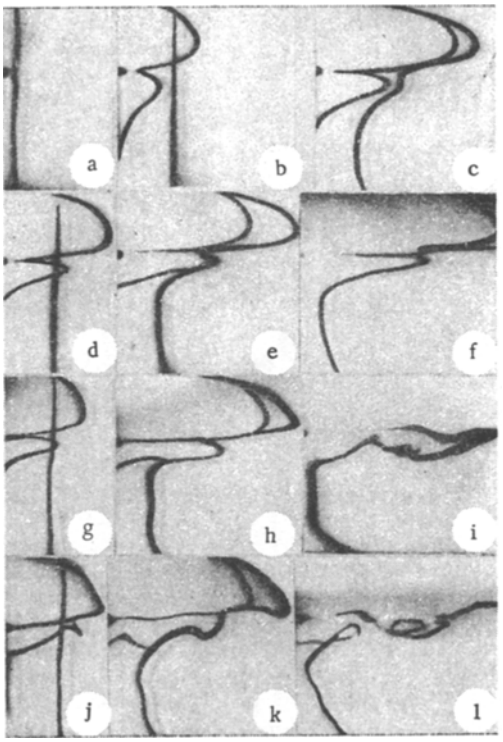

Fig. 5

the film (thickness) ranged from 0.07 to 0.03 cm, while the width was a constant 3 mm for the entire section.

To check for the absence of convective motion of the markings as a result of local heating by the laser radiation, we filmed the markings in still liquid. An analysis of the resulting data showed that the markings did not move for periods of up to 2 sec. The motion of the photo-induced markings in the flow was photographed in less than 2 sec. During this time, the markings moved downstream for distances up to 5 cm until they left the observation zone. To measure the displacement of the markings relative to their initial position, the resulting negatives were projected on a screen. Figure 3 shows results of visualization of the motion of liquid in a pipe without an obstacle. The figure shows photographs of the position of a linear colored marking in the flow for different Reynolds numbers at different moments of time t after photostimulation (a-c correspond to Re = 1000, t = 0.015, 0.125, 0.245 sec; d-f, Re = 1648, t = 0.09, 0.11, 0.13 sec; g-i, Re = 2400, t = 0.065, 0.07, 0.07 sec).

In the experiments, the laser beam was directed vertically from top to bottom over the diameter of the pipe. We began to count time from the moment the beam formed, when it was rectilinear. The velocity distribution shown in Fig. 3a-c has a parabolic form. These photographs were reproduced with an accuracy lying within the measurement error each time the experimental conditions were reproduced.

It should be noted that a series of preliminary experiments showed that the form of the parabolic velocity distribution in the flow is highly sensitive to the accuracy of joining of the working and auxiliary sections of the cylindrical channel of the stand. A small misalignment in the joint led to shifting of the vertex of the parabola away from the pipe axis. Thus, when we conducted the experiments we took special steps to precisely monitor the coaxiality of all sections of the channel.

Figure 4a compares the velocity distributions (Fig. 3a-c) with the theoretical Poiseuille profile for Re = 1000. It is evident that at Re = 1000 the distribution (curve 2) coincides with the velocity distribution according to the Poiseuille law (curve 1) within the empirical error, determined by the thickness of the colored lines.

The character of flow in the pipe changes with an increase in the discharge to values corresponding to Re > 1000. The velocity distribution in the cross section ceases to be parabolic and is no longer constant over time. The photographs in Fig. 3d-f were obtained 0.09, 0.11, and 0.13 sec after the creation of the rectilinear marking in the flow. The discharge was constant in each case and corresponded to Re = 1648. The series of photographs in Fig. 3g-i was obtained in a flow with a constant discharge at Re = 2400. It is evident that an increase in flow velocity is accompanied by the development of instability in the central part of the flow, and the size of the unstable flow region increases with an increase in Re. The time interval between the series of photographs was several minutes.

Evaluation of the distance until the establishment of the Poiseuille profile in the circular pipe from the formula [6] $\ell_{ini} = 0.024(2d)\mathrm{Re}$ shows that the distance ℓ = 1130 mm, separating the working section from the channel inlet, satisfies the inequalities $\ell > \ell_{ini}$ at Re = 1000 and $\ell < \ell_{ini}$ at Re = 1648, 2400. These estimates agree with the experimental data.

To avoid the development of transience in the inlet part of the channel, when studying flow about the obstacle we kept the discharge in the system at a constant value corresponding to Re ≤ 1000. The obstacle was located in the section at a distance of ℓ = 1130 mm from the inlet. The location of the obstacle secured in the pipe is shown schematically in Fig. 4b.

The unit we used allowed us to obtain colored markings in two different sections either simultaneously or with a time shift, which in turn made it possible to obtain intersecting lines and to use the displacements of the points of intersection to evaluate fluid velocity in the radial direction.

Flow about the obstacle was studied at Re = 188, 377, 572, 774, and 1000. Figure 5 shows results from flow visualization in the pipe after the obstacle for different Re with the use of two markings. The first linear colored marking was created in a section located 1 mm from the top of the upper half-disk. The second marking, time-shifted by an amount equal to Δt, was located in a section 10 mm downstream. The lag time Δt associated with the formation of the marking in the second section was chosen so that the two markings intersected in the second section.

Figure 5 shows several typical examples of frames obtained in the experiments to show the markings at different moments of time in the flow behind the obstacle at different Re. The values of Re and the times corresponding to the photographs are shown in Table 1, where t_1 and t_2 are the moments the first and second markings were photographed. These moments were reckoned from the moments the markings were induced. The quantity Δt in Table 1 is the time interval between the moments the first and second markings were induced.

The motion of the photo-induced markings was recorded at a speed of 100 frames/sec. The time of exposure was $4 \cdot 10^{-3}$ sec. The duration of the laser pulse was $8 \cdot 10^{-4}$ sec and determined the moment of formation of the colored marking. The time between two frames was 10^{-2} sec. The moment of formation of the colored marking could have fallen in the time interval between frames, which usually resulted in the formation of a nonrectilinear marking deformed by the flow on the first frame. Since we synchronized the time of recording of the camera operation and the moments of formation of the colored markings, this phenomenon did not affect the accuracy of determination of the time intervals between the moment of marking formation and the moment the marking was recorded on the camera. These intervals were $5 \cdot 10^{-3}$ sec [5].

TABLE 1

Fig. 5	t_1	Δt	t_2	Re	Fig. 5	t_1	Δt	t_2	Re
a	0			188	g	0,115	0,105	0,01	572
b	0,265	0,255	0,01	188	h	0,255	0,105	0,16	572
c	0,615	0,255	0,36	188	i	0,515	0,105	0,41	572
d	0,21	0,2	0,01	377	j	0,09	0,085	0,005	774
e	0,375	0,2	0,175	377	k	0,185	0,085	0,1	774
f	0,55	0,2	0,35	377	ℓ	0,28	0,085	0,195	774

The data – only a small part of which is shown in Fig. 5 – give a range of information on the hydrodynamics of the flow beyond the barrier and makes it possible to establish the structure of the flow and break it down into stream and stagnant regions, determine the beginning of transience in the flow, study the character of the flow, and detect vortical structures in the mixing region. It is evident in particular that the flow beyond the obstacle breaks down into three main regions: upper and central regions of stream flow and a stagnant region in the lower part of the flow. Also, motion of the fluid along the bottom wall of the channel is visible in the photographs. This motion is connected with the loose contact between the bottom disk and the channel surface. This gap increases in size with an increase in the discharge. The recording of the motion of fluid through small gaps by the PCV method might be used to measure the size of gaps in complicated contacts [7].

The form of each region and the velocity distribution in them depend on Re. At Re = 188 and 377, the flow in the streams, the mixing region, and the stagnant region remains laminar and steady over the entire recorded field, i.e., up to 30 mm from the top of the upper half-disk. Unstable flow is seen at Re = 572 in the mixing region of the top stream and on the boundary between the central stream and the reverse-velocity region. The unstable flow is characterized by the formation of closed circulation zones which form a vortex street that begins 10 mm from the point of convergence of the streams from the edge of the half-disk separating the flow. With a further increase in Re (see Fig. 5 j, k, ℓ), the trailing vortex approaches the edge of the half-disk, the mixing region embraces a larger part of the regions of stream flow, and the eddies become more powerful and penetrate deeper into the stagnant zone. At Re = 1000, pronounced instability is evident in the flow at just 6 mm from the edge of the ring of the upper half-disk.

It should be noted that the flow remains steady and close to unidirectional in the investigated range of Re in the immediate vicinity of the plane of the upper half-disk. Thus, the data obtained on the displacement of the linear marking in this region can be used to calculate the velocity field of the liquid. The velocity distribution in the flow section 1 mm from the top of the upper half-disk, calculated from data from the photochromic visualization, is shown in Fig. 4. These results can also be used to calculate the shear stresses on the walls and in the body of the flow.

Thus, the method of photochromic visualization proves to be quite effective for studying features of liquid flows with a complex geometry at moderate Re. Use of the method will be expedient in problems concerning the character of motion of a liquid in a gap between two parallel surfaces [8], flow through a slit [9], etc.

LITERATURE CITED

1. V. A. Al'vares-Suares, V. A. Barachevskii, et al., "Method of photochromic visualization of hydrodynamic flows," Preprint IPM AN SSSR, No. 203, Moscow (1982).
2. V. A. Barachevskii, V. F. Mandzhikov, et al., "Photochromic method of visualizing hydrodynamic flows," Zh. Prikl. Mekh. Tekh. Fiz., No. 5 (1984).
3. A. Palade de Iribarne, R. L. Hummel, et al., "Transition turbulent flow parameters in a smooth pipe by direct flow visualization," Chem. Eng. Prog., 5, No. 91 (1969).
4. V. G. Dmitriev and L. V. Tarasov, Applied Nonlinear Optics [in Russian], Radio i Svyaz', Moscow (1982).
5. V. N. Yurechko, Yu. S. Ryazantsev, et al., "Study of the hydrodynamic characteristics of liquid flows by the method of photochromic visualization," Preprint, IPM AN SSSR, No. 263, Moscow (1985).
6. H. Schlichting, Boundary Layer Theory, 7th ed., McGraw-Hill (1979).

7. A. S. Bukatov, N. A. Iofis, Yu. V. Martynov, Yu. S. Ryazantsev, and V. N. Yurechko, "Method of measuring gaps," USSR Inventor's Certificate No. 1170271; Byull. Izobret., No. 28 (1985).
8. V. E. Nakoryakov, O. N. Kashinskii, et al., "Study of a jet flow propagating between two parallel walls," Zh. Prikl. Mekh. Tekh. Fiz., No. 1 (1985).
9. V. D. Zhak, V. A. Mukhin, et al., "Propagation of a submerged jet in a narrow slit," Zh. Prikl. Mekh. Tekh. Fiz., No. 3 (1985).

HOLOGRAPHIC STUDY OF FLOWS WITH PHOTOCHROMIC VISUALIZATION

Zh. S. Akylbaev and A. O. Tseeb

UDC 532.574

To measure the velocity and temperature profiles in a fluid flow, we chose two nondisturbing optical methods: the method of interferometry [1] to measure the temperature profile; the method of a holographic photochromic fluid to measure the velocity profile. Certain changes were made to the latter method in order to allow the two methods to be used together. These changes were specifically dictated by the fact that the photochromic liquid chosen in [2] was an alcohol solution of a substance, belonging to the class of spiropyrans, which changes color from transparent to red under the influence of ultraviolet radiation. However, the colored marking has a low contrast and requires special bias lighting, i.e., it is necessary to choose the wavelength of the bias light source.

The use of such a photochromic liquid for studies in a boundary layer is generally complicated by the fact that with magnification of the colored part of the liquid by the optical system, such as a microscope, contrast is lost at the boundary of the marking. This loss of contrast continues up to a magnification of about 50, when the marking disappears altogether. This leads to errors in the measurement of the coordinates of the colored wake and, thus, in the measurement of velocity in the boundary layer. We should also note the high cost of spiropyrans and the complexity of preparing aqueous solutions of the photochromic liquid. Moreover, a photochromic reaction of this type is reversible, and the colored marking exists for only a limited time. To avoid these problems and, more important, to permit recording of the colored marker against a background of red laser radiation – necessary to simultaneously study the temperature field – we used an aqueous solution of potassium ferrioxalate as the photochromic liquid.

This allowed us to obtain a highly contrasting colored marking noticeable against the entire visible spectrum. This in turn made it possible to use radiation from a helium–neon or ruby laser as the bias lighting. In addition, the contrast of the marking does not diminish with an increase in the magnification of the optical system, which means that it is possible to conduct investigations in boundary layers. In contrast to spiropyrans, dissolvable only in organic liquids, the ability of potassium ferrioxalate to dissolve in water permits simplification of the process of preparing aqueous solutions of the photochromic liquid and allows its viscosity to be varied through the addition of glycerin or sugar. Other important advantages of this method are the availability and low cost of the chemical components of the photochromic liquid when potassium ferrioxalate is used.

A working solution of the photochromic liquid was prepared by dissolving potassium ferrioxalate in water with an addition of sulfuric acid. In an acid solution, ferrioxalate ions dissociate into mono- and dioxalate complexes. Exposure to light produces ions of bivalent iron:

$$[Fe(C_2O_4)]^+ \xrightarrow{h\nu} Fe^{2+} + (C_2O_4)^-,\ (C_2O_4)^- + [Fe(C_2O_4)]^+ \rightarrow 2CO_2 + Fe^{3+} + (C_2O_4)^{2-}.$$

Karaganda. Translated from Zhurnal Prikladnoi Mekhaniki i Tekhnicheskoi Fiziki, No. 5, pp. 19-23, September-October, 1987. Original article submitted May 28, 1986.

0021-8944/87/2805-0659$12.50